



Published in final edited form as:

ACS Macro Lett. ; 2(9): . doi:10.1021/mz400229m.

## Construction of a Reactive Diblock Copolymer, Polyphosphoester-*block*-Poly(L-lactide), as a Versatile Framework for Functional Materials that are Capable of Full Degradation and Nanoscopic Assembly Formation

Young H. Lim, Gyu Seong Heo, Sangho Cho, and Karen L. Wooley\*

Departments of Chemistry and Chemical Engineering, Texas A&M University, College Station, Texas 77842, United States

### Abstract

The development of a diblock copolymer, polyphosphoester-*block*-poly(L-lactide), which has potential for being fully-degradable and biocompatible, was achieved by one-pot sequential ring-opening polymerizations (ROPs) of two cyclic monomers: alkyne-functionalized phospholane and L-lactide (LLA). A kinetic study of the polymerization in each step was investigated in a detailed manner by nuclear magnetic resonance (NMR) spectroscopy and gel permeation chromatography (GPC), revealing living/controlled characteristics with narrow molecular weight distributions and a linear increase of molecular weights vs. monomer conversion and time. Subsequently, photo-induced thiol-yne “click” reactions with small molecule thiols bearing either carboxylic acid or amino groups afforded amphiphilic diblock copolymers with carboxylate or amino side-chain functionalities along the polyphosphoester segment of the diblock copolymer backbone. Finally, direct dissolution of the two different types of amphiphilic diblock copolymers in aqueous solutions yielded well-defined spherical micelles with corresponding negative or positive surface charges, respectively, as confirmed by transmission electron microscopy (TEM), dynamic light scattering (DLS) and zeta potential analyses.

---

The use of hydrocarbon backbone-based polymers in the development of polymeric nanoconstructs is a well-established concept in nanomedicine, but toxicity, immunogenicity and other side effects from long-time accumulation in the human body is often an inevitable bottleneck in the field of therapeutics, imaging, diagnostics and drug delivery.<sup>1</sup> To overcome this fatal drawback, hydrolytically-degradable polymers such as polyesters and polycarbonates have been studied as potential biomaterials owing to their low toxicity, biocompatibility and degradability.<sup>2,3</sup>

In spite of their great promises in nanomedicine, elaborate synthetic approaches due to difficulties experienced in controlling polymerizations, challenges in the introduction of functionalities, incompatibilities of desired functionalities with polymerization methods, and tedious work-up processes often present challenges towards developing well-defined, functional degradable biomaterials.<sup>4-6</sup> A broad range of organocatalysts have been studied extensively in ring-opening polymerizations (ROPs),<sup>7-10</sup> which offer controllability while

---

\*Corresponding Author: wooley@chem.tamu.edu.

#### SUPPORTING INFORMATION

Detailed experimental procedures including monomer and polymer synthesis, post-polymerization modification, nanoparticle preparation, and characterization. The material is available free of charge via the Internet at <http://pubs.acs.org>.

Supporting Information Placeholder

avoiding potential purification issues and biological complications of the traditional metal-based catalyst systems.<sup>11,12</sup> Although there are exceptions,<sup>13</sup> the introduction of side chain functionalities into the cyclic monomers commonly involves multistep reactions. In contrast, cyclic phospholanes offer a straightforward, single-step installation of reactive functionalities that are compatible with the ROP conditions and also provide opportunities for diverse post-polymerization modification reactions, including “click”-type reactions.<sup>14–18</sup> Introducing these “clickable” functionalities onto cyclic monomers is of particular interest with respect to the synthetic approach to degradable polymers, as this sequence of chemistry would not only broaden the synthetic versatility but also enable the construction and fabrication of intricate polymeric nanoparticles for pharmaceutical applications.<sup>14,15</sup>

“Hybrid” polymers can provide a mechanism to accommodate disparate physical, chemical and mechanical advantages from diverse polymer segments.<sup>19–22</sup> Particularly, integrating heterogeneous degradable polymers into one polymeric system is expected to enhance the combinatorial effects on the development of versatile polymer frameworks, which is often limited in the case of a single-type copolymer backbone system. Among important biomedical degradable polymers, polylactide (PLA)<sup>23–26</sup> is an interesting building block for the construction of functional nanoscopic objects, due to its capability for hydrolytic and/or enzymatic degradation and several elegant works on the formation of well-defined polymeric nanostructures with distinctive core-shell morphologies and higher-order complexities based on the adaptation of the intrinsic hydrophobicity and crystallinity of PLAs within amphiphilic block copolymers.<sup>27–30</sup> Therefore, we have combined our recent exploration into a rapid and facile construction of nanostructures derived from a biomimetic polyphosphoester<sup>31–35</sup>-based block copolymer system<sup>14,15</sup> with PLA.

The first attempt to prepare a diblock copolymer of L-lactide (LLA) and phospholane, PLLA-*b*-PPE, was made by Wang *et al.*;<sup>36</sup> however, it required demanding two-step polymerizations using metal catalyst, Sn(Oct)<sub>2</sub>, and no functional moieties were incorporated into the polymeric system. In this report, we demonstrate the preparation of fully-degradable, hybrid, functional diblock copolymers by one-pot sequential ROPs of two different kinds of cyclic monomers, phospholane and LLA, using an organocatalyst, 1,8-diazabicyclo[5.4.0]undec-7-ene (DBU). This platform was, subsequently, modified by a radical-mediated “click”-type thiol-yne reaction to endow charges and functional side-chain moieties to the polyphosphoester (PPE) segment. The obtained functionalized diblock copolymers, in turn, were demonstrated to self-assemble into well-defined spherical nanoparticles in aqueous solutions with corresponding surface charges, as characterized by transmission electron microscopy (TEM), dynamic light scattering (DLS) and zeta potential analyses.

Compared to our previous reports, in which sequential ROPs of two phospholanes were conducted at different temperatures on a Schlenk line, the ROPs of butynyl phospholane (BYP, **1**)<sup>15</sup> and LLA were performed in a one-pot manner in a glove box, at ambient temperature and with convenience in the elimination of potential introduction of water as a competitive initiator. In an initial study, homopolymer, PBYP, was prepared by employing DBU as the organocatalyst and benzyl alcohol as the initiator (Scheme 1). The conversion reached up to 95% with a low polydispersity index (PDI~1.2) within 7 min in dichloromethane (CH<sub>2</sub>Cl<sub>2</sub>). After this initial screening reaction, kinetic studies of each sequence of the polymerizations in the glove box were performed.

For the kinetic studies, BYP and benzyl alcohol (molar ratio of 50 : 1) were mixed in CH<sub>2</sub>Cl<sub>2</sub>, DBU (molar ratio to initiator of 2 : 1) was added, and the polymerizations were monitored. After being stirred for a predetermined period of time, an aliquot of the reaction

mixture was collected, quenched by addition of a solution of benzoic acid in  $\text{CH}_2\text{Cl}_2$ , and then analyzed by  $^{31}\text{P}$  NMR spectroscopy and GPC (Figure S1). While the conversions were calculated from  $^{31}\text{P}$  NMR spectroscopy by comparing the integral ratios of two distinct peaks of monomer, **1**, at 17.34 ppm and homopolymer, PBYP, at  $-1.60$  ppm, both the molecular weight and its distribution were determined by GPC. The GPC molecular weight values were of low accuracy because they are based on calibration with polystyrene standards; however, we believe that the molecular weight distributions are representative of the controlled nature of the polymerizations. Polymerization proceeded rapidly, in which the monomer conversion reached to 67% within the beginning 2 min. The maintenance of linearity of  $M_n$  vs. monomer conversion suggested a living ROP up to 95%. The PDIs were less than 1.30, and even lower PDI values ( $<1.20$ ) were obtained when the monomer conversion was  $<95\%$ . The increased PDI at higher monomer conversions could be attributed to adverse transesterification of the polyphosphoester backbone. Kinetic plots of  $\ln([M]_0/[M])$  vs. time indicated pseudofirst order kinetics, which are a typical characteristic of ROP. The degrees of polymerization (DP) calculated based on  $^{31}\text{P}$  NMR spectroscopy-determined monomer conversions agreed with those calculated from chain-end analysis by  $^1\text{H}$  NMR spectroscopy; that is, by comparisons of the integrals of proton resonances of the benzyl group (7.42–7.30 ppm) of the initiated chain end to those of the PBYP backbone (4.34–4.22 ppm) or those of the - and -protons on the substituents (4.22–4.08 ppm and 2.67–2.56 ppm, respectively).

PBYP was extended with PLLA *via* a one-pot sequential polymerization method, which provides a facile strategy to prepare diblock copolymers with structural control in an atomefficient and labor-saving approach. It is noteworthy that the ROP rate of phospholanes is strongly dependent on the monomer and organocatalyst concentrations.<sup>15</sup> Therefore, we speculated that manipulations of monomer concentration in solution would enable the construction of diblock copolymers, while maintaining a high efficiency of ROP of two cyclic monomers sequentially, each using DBU. For this reason, ROP of LLA was conducted after the formation of the PPE block. That is, when the concentration of BYP in the initial polymerization mixture was diluted from 5.7 M to 0.28 M after consumption of 95% of BYP and further to 0.036 M, and the DBU concentration was reduced from 0.23 M to 0.028 M upon the addition of the second monomer solution in  $\text{CH}_2\text{Cl}_2$ , the rate of BYP polymerization slowed to an immeasurable level, as confirmed by  $^{31}\text{P}$  NMR spectroscopy. Therefore, addition of LLA in  $\text{CH}_2\text{Cl}_2$  promoted an extension of the second block while preventing further growth of PBYP.

The kinetic study showed that the chain extension of PLLA was achieved within a few minutes with good control (Figure 1). At 7 min of polymerization of BYP (after which a rapid increase in PDI was shown), a solution of LLA in  $\text{CH}_2\text{Cl}_2$  was quickly added into the reaction mixture. An aliquot of the reaction solution was collected, quenched and analyzed by  $^1\text{H}$  NMR spectroscopy and GPC. The conversion of LLA had reached 90% with a low PDI ( $\sim 1.2$ ) after 4 min. A linearity of  $M_n$  vs. monomer conversion was observed during polymerization, up to 80% conversion with low PDIs ( $<1.20$ ). Similar to the polymerization of BYP, the kinetic plots of  $\ln([M]_0/[M])$  vs. time for LLA chain extension showed pseudo-first-order kinetics.

A scaled-up production of **2** was then conducted using the same molar ratios as used for the kinetic studies, followed by precipitation in diethyl ether for purification. The DP values were determined by  $^1\text{H}$  NMR and  $^{31}\text{P}$  NMR spectroscopy endgroup analysis and monomer conversion calculations, respectively. Furthermore, the integral ratios between the peak of the terminal acetylene proton (2.28–2.09 ppm) within the PBYP block and that of the methine or methyl protons on the PLLA block were consistent, which was indicative of retention of the alkyne groups. In addition, one distinct  $^{31}\text{P}$  resonance confirmed the stability

of the degradable PPE backbone during the ROP of LLA and isolation and characterization of the block copolymer. GPC analysis of the diblock copolymer showed a mono-modal peak with PDI of 1.17.

To afford positive or negative charges along the backbone of one segment of the diblock copolymer, in the construction of amphiphilic block copolymers, thiol-yne “click” reactions were conducted to couple two different kinds of thiol-containing compounds onto the PPE block. The radical-mediated thiol-yne “click” chemistry is a robust and versatile method that tolerates a variety of functional groups in achieving a high degree of functionalization on alkyne groups.<sup>37,38</sup> Herein, this efficient click chemistry was applied to achieve double addition of small molecules at each PPE repeat unit by coupling two equivalents of thiols onto one alkyne moiety. This double-conjugation of molecules onto the hydrophilic segment would maximize the number of functionalities as well as the solubility of the amphiphilic diblock copolymers in water. In order to confirm the integrity of the polyphosphoester and poly(L-lactide) backbones under the presence of radicals and UV irradiation, a mixture of polymer and 2,2-dimethoxy-2-phenylacetophenone (DMPA) as a photoinitiator in dimethyl sulfoxide-d<sub>6</sub> (DMSO-d<sub>6</sub>) were irradiated under UV light (365 nm, 6 W) for several hours, as a preliminary control reaction. Both <sup>1</sup>H and <sup>31</sup>P NMR spectra demonstrated that all of the functional groups and polymer back-bones were intact under these conditions. Accordingly, ten molar equivalents of thiols relative to alkynes were employed in the radical reaction to avoid possible chain-chain coupling and to ensure a high coupling efficiency. 3-Mercaptopropionic acid and 2-aminoethanethiol were chosen because of their commercial availability and the potential self-assembly into anionic or cationic nanoparticles from the resulting negatively- or positively-charged amphiphilic block copolymers, respectively.

Figure 2 shows a comparison of <sup>1</sup>H and <sup>31</sup>P NMR spectra of PPE<sub>49</sub>-*b*-PLLA<sub>44</sub> before and after thiol-yne “click” reactions. The approximately complete disappearance of the terminal acetylene proton (labeled as g in Figure 2(a)), coincident with the emergence of distinguishable diastereotopic methylene protons (labeled as k in Figures 2(b) and 2(c)) confirmed the conversion of alkynyl groups into the corresponding 1,2-dithioether functional groups.

The self-assembly behaviors of the two amphiphilic diblock copolymers, **3** and **4**, were studied by direct dissolution in buffer solution. **3** and **4** were dissolved and stirred for 10 min in 3-(*N*-morpholino)propanesulfonic acid (MOPS) buffer solution (pH 7.4, 150 mM) and acetate buffer solution (pH 5.0, 150 mM), respectively, with polymer concentrations of 1.0 mg/mL. The morphologies of the resulting nanoparticles having different charges within their hydrophilic shells were characterized by DLS and TEM (Figure 3). DLS results indicated narrow and mono-modal size distributions of anionic and cationic nanoparticles. For **5**, the number-average hydrodynamic diameter was *ca.* 25 nm. The number-average hydrodynamic diameter of **6** was *ca.* 16 nm. Similarly, TEM images of **5** and **6** also showed uniform particles with average sizes of approximately 18 nm and 16 nm, respectively.

The surface charge densities of **5** and **6** in buffer solutions at pH 5.0 and 7.4 were measured as zeta potential values (Figure S2). As predicted, **5** were negatively charged with zeta potentials of -16.9 mV at pH 5.0 and -25.5 mV at pH 7.4, and **6** were positively charged, showing zeta potential values of +31.4 mV at pH 5.0 and +26.0 mV at pH 7.4. The distinct difference in zeta potential values demonstrated the presence of surface charges on the micelles as well as the potential utilization of functionalities for further modifications.

In conclusion, a versatile platform for the construction of spherical micelles with different surface charges and functionalities based on fully-degradable, hybrid diblock copolymer, PPE-*b*-PLLA, was developed. First, well-defined (PDI <1.2) diblock copolymers of alkyne-

functional phospholanes and L-lactides were prepared by conducting rapid and facile one-pot sequential ROPs using an organocatalyst, DBU. The kinetic study of each block polymerization demonstrated an excellent controllability during ROP. Subsequently, photoinitiated, radical-mediated thiol-yne “click” chemistry was employed to convert the parental hydrophobic diblock copolymer into amphiphilic diblock polymers with different side chain functionalities. Finally, the direct dissolution of the amphiphilic diblock copolymers in water promoted the formation of well-defined spherical nanoparticle assemblies with distinct negative and positive surface charges and uniform size distributions, as characterized by TEM, DLS and zeta potential analyses. The fundamental understanding of degradability of these diblock copolymers and the application of nanoparticles in nanomedicine are currently under investigations.

## Supplementary Material

Refer to Web version on PubMed Central for supplementary material.

## Acknowledgments

We gratefully acknowledge financial support from the National Heart Lung and Blood Institute as a Program of Excellence in Nanotechnology (HHSN268201000046C) and from the National Institute of Diabetes and Digestive and Kidney Diseases (R01-DK082546). The Welch Foundation is gratefully acknowledged for support through the W. T. Doherty-Welch Chair in Chemistry, Grant No. A-0001.

## References

1. Langer R. *Science*. 1990; 249:1527. [PubMed: 2218494]
2. Nederberg F, Zhang Y, Tan JPK, Xu K, Wang H, Yang C, Gao S, Guo XD, Fukushima K, Li L, Hedrick JL, Yang YY. *Nat Chem*. 2011; 3:409. [PubMed: 21505501]
3. Kang N, Perron M-É, Prud'homme RE, Zhang Y, Gaucher G, Leroux JC. *Nano Lett*. 2005; 5:315. [PubMed: 15794618]
4. Yu Y, Zou J, Yu L, Ji W, Li Y, Law WC, Cheng C. *Macromolecules*. 2011; 44:4793.
5. Zhang X, Zhong Z, Zhuo R. *Macromolecules*. 2011; 44:1755.
6. Xu J, Prifti F, Song J. *Macromolecules*. 2011; 44:2660. [PubMed: 21686053]
7. Csihony S, Culkin DA, Sentman AC, Dove AP, Waymouth RM, Hedrick JL. *J Am Chem Soc*. 2005; 127:9079. [PubMed: 15969586]
8. Dove AP, Pratt RC, Lohmeijer BGG, Waymouth RM, Hedrick JL. *J Am Chem Soc*. 2005; 127:13798. [PubMed: 16201794]
9. Kang HU, Yu YC, Shin SJ, Kim J, Youk JH. *Macromolecules*. 2013; 46:1291.
10. Coady DJ, Engler AC, Horn HW, Bajjuri KM, Fukushima K, Jones GO, Nelson A, Rice JE, Hedrick JL. *ACS Macro Lett*. 2011; 1:19.
11. Kamber NE, Jeong W, Waymouth RM, Pratt RC, Lohmeijer BGG, Hedrick JL. *Chem Rev*. 2007; 107:5813. [PubMed: 17988157]
12. Hild F, Neehaul N, Bier F, Wirsum M, Gourlaouen C, Dagorne S. *Organometallics*. 2013; 32:587.
13. Tempelaar S, Barker IA, Truong VX, Hall DJ, Mespouille L, Dubois P, Dove AP. *Polymer Chemistry*. 2013; 4:174.
14. Zhang S, Zou J, Zhang F, Elsabahy M, Felder SE, Zhu J, Pochan DJ, Wooley KL. *J Am Chem Soc*. 2012; 134:18467. [PubMed: 23092249]
15. Zhang S, Li A, Zou J, Lin LY, Wooley KL. *ACS Macro Lett*. 2012; 1:328. [PubMed: 22866244]
16. Wang YC, Yuan YY, Wang F, Wang J. *J Polym Sci, Part A: Polym Chem*. 2011; 49:487.
17. Liu J, Huang W, Pang Y, Zhu X, Zhou Y, Yan D. *Biomacromolecules*. 2010; 11:1564. [PubMed: 20364861]
18. Iwasaki Y, Akiyoshi K. *Macromolecules*. 2004; 37:7637.

19. Thurn-Albrecht T, Schotter J, Kästle GA, Emley N, Shibauchi T, Krusin-Elbaum L, Guarini K, Black CT, Tuominen MT, Russell TP. *Science*. 2000; 290:2126. [PubMed: 11118143]
20. Bates FS, Hillmyer MA, Lodge TP, Bates CM, Delaney KT, Fredrickson GH. *Science*. 2012; 336:434. [PubMed: 22539713]
21. Li B, Li L, Wang B, Li CY. *Nat Nanotechnol*. 2009; 4:358. [PubMed: 19498396]
22. Warren SC, Messina LC, Slaughter LS, Kamperman M, Zhou Q, Gruner SM, DiSalvo FJ, Wiesner U. *Science*. 2008; 320:1748. [PubMed: 18583606]
23. Jeong B, Bae YH, Lee DS, Kim SW. *Nature*. 1997; 388:860. [PubMed: 9278046]
24. Dimitrov IV, Berlinova IV, Michailova VI. *Polym J*. 2013; 45:457.
25. Samarajeewa S, Ibricevic A, Gunsten SP, Shrestha R, Elsabahy M, Brody SL, Wooley KL. *Biomacromolecules*. 2013; 14:1018. [PubMed: 23510389]
26. Samarajeewa S, Shrestha R, Li Y, Wooley KL. *J Am Chem Soc*. 2011; 134:1235. [PubMed: 22257265]
27. Yamamoto Y, Yasugi K, Harada A, Nagasaki Y, Kataoka K. *J Control Release*. 2002; 82:359. [PubMed: 12175749]
28. Sun J, Chen X, Lu T, Liu S, Tian H, Guo Z, Jing X. *Langmuir*. 2008; 24:10099. [PubMed: 18698858]
29. Petzetakis N, Dove AP, O'Reilly RK. *Chem Sci*. 2011; 2:955.
30. Ting SRS, Gregory AM, Stenzel MH. *Biomacromolecules*. 2009; 10:342. [PubMed: 19159200]
31. Xiong MH, Bao Y, Yang XZ, Wang YC, Sun B, Wang J. *J Am Chem Soc*. 2012; 134:4355. [PubMed: 22304702]
32. Lapienis G, Penczek S, Pretula J. *Macromolecules*. 1983; 16:153.
33. Wang YC, Yuan YY, Du JZ, Yang XZ, Wang J. *Macromol Biosci*. 2009; 9:1154. [PubMed: 19924681]
34. Iwasaki Y, Yamaguchi E. *Macromolecules*. 2010; 43:2664.
35. Clément B, Grignard B, Koole L, Jérôme C, Lecomte P. *Macromolecules*. 2012; 45:4476.
36. Yang XZ, Sun TM, Dou S, Wu J, Wang YC, Wang J. *Biomacromolecules*. 2009; 10:2213. [PubMed: 19586040]
37. Hoyle CE, Bowman CN. *Angew Chem Int Ed*. 2010; 49:1540.
38. Iha RK, Wooley KL, Nystrom AM, Burke DJ, Kade MJ, Hawker CJ. *Chem Rev*. 2009; 109:5620. [PubMed: 19905010]

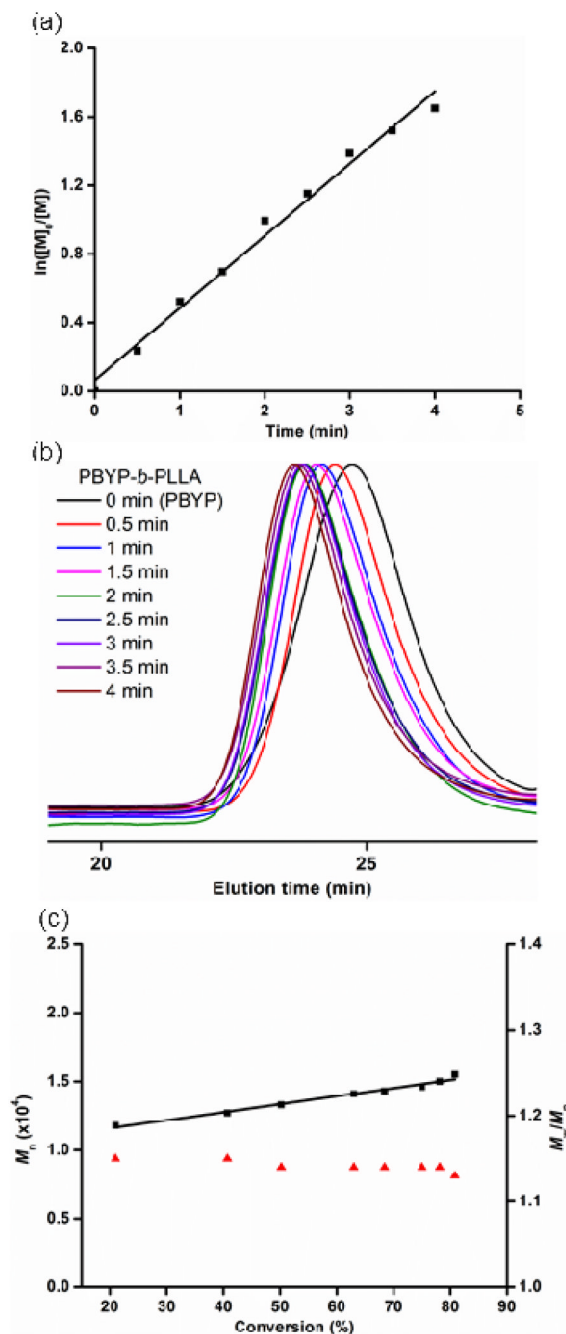


**Figure 1.**

(a) Kinetic plots of  $\ln([M]_0/[M])$  vs. time, obtained from  $^1\text{H}$  NMR spectroscopy data. (b) GPC traces (DMF as eluent, 1 mL/min) as a function of polymerization time, for the chain extension of LLA to PBYP after a solution of LLA in  $\text{CH}_2\text{Cl}_2$  was added at 7 min of homopolymerization of BYP. (c) Kinetic plots of  $M_n$  and  $M_w/M_n$  vs. monomer conversion, obtained from GPC analysis, during the chain extension of PBYP with PLLA *via* one-pot sequential ROPs. Conditions:  $[\text{LLA}] = 0.72 \text{ M}$  in  $\text{CH}_2\text{Cl}_2$ ,  $[\text{LLA}] : [\text{PBYP}] = 50 : 1$ .

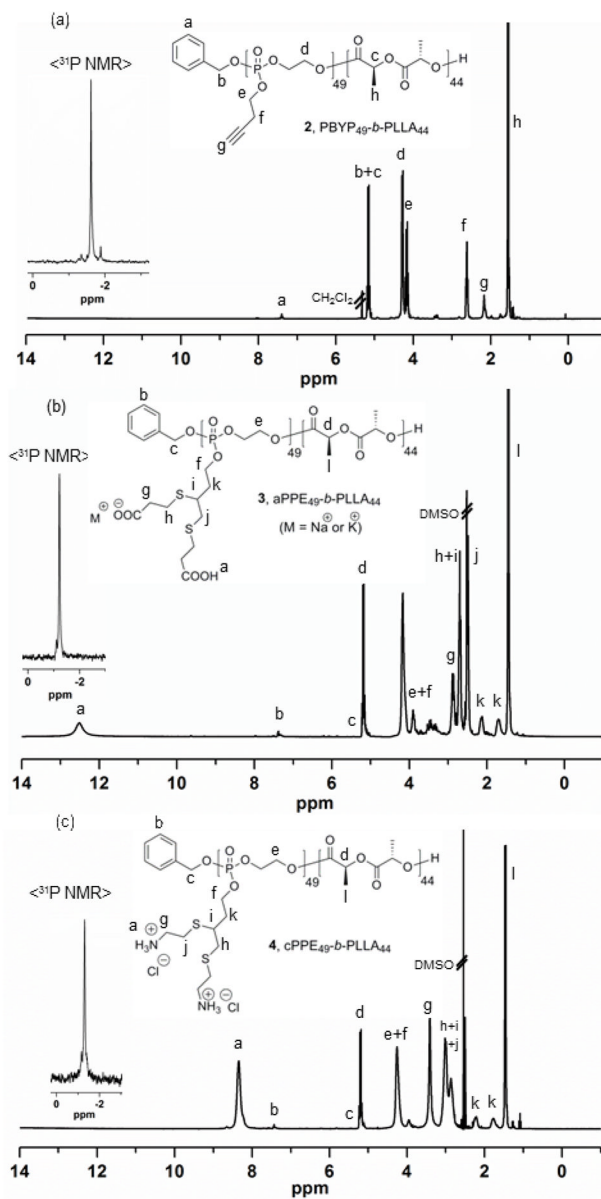


**Figure 2.**  $^1\text{H}$ - and  $^{31}\text{P}$ -NMR spectra of **2** (a), and product polymers after thiol-yne reactions, **3** (b) and **4** (c).



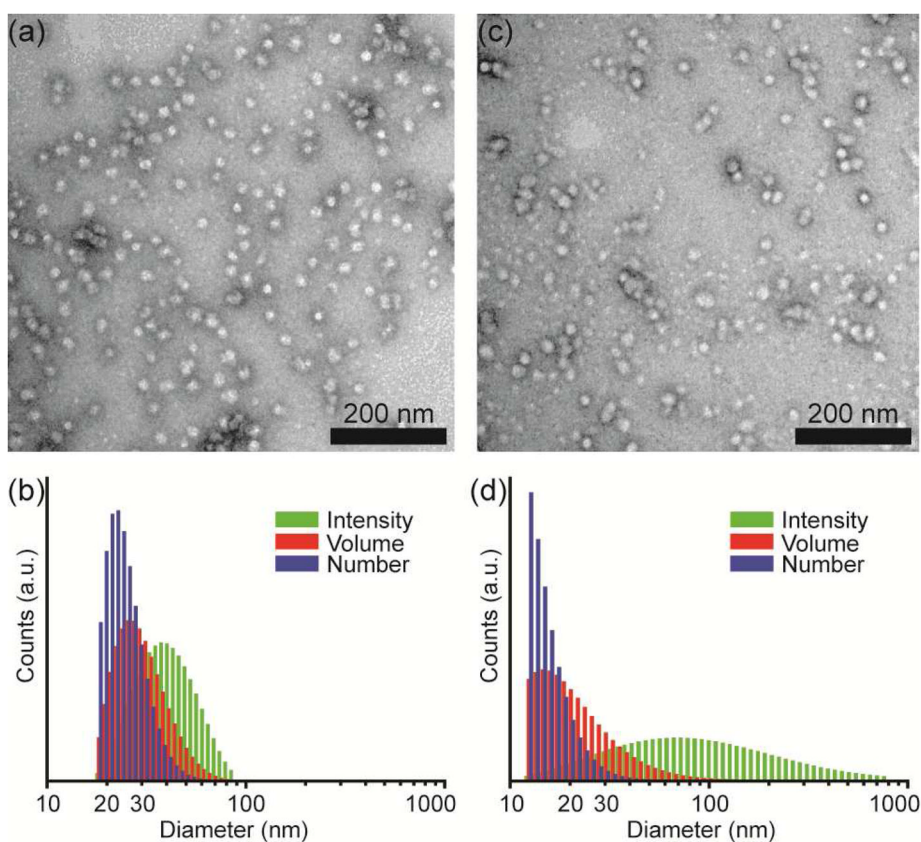
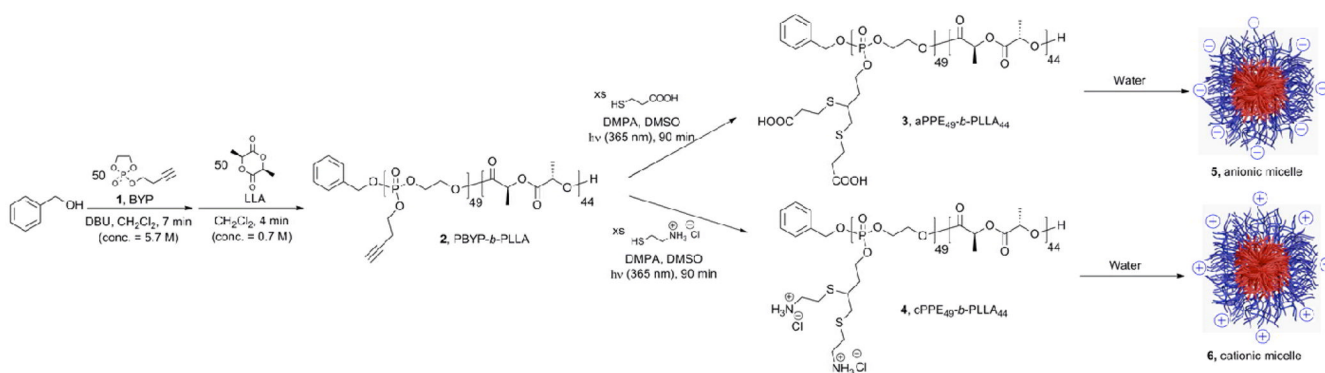


**Figure 3.** Self-assembly results of anionic micelle **5** (a and b) and cationic micelle **6** (c and d) in MOPS buffer at pH 7.4 and acetate buffer at pH 5.0, respectively. (a) TEM image of **5**:  $D_{av} = 18 \pm 3$  nm, after counting more than 150 nanoparticles. (b) DLS results of **5**:  $D_{h(intensity)} = 41 \pm 14$  nm,  $D_{h(volume)} = 31 \pm 10$  nm and  $D_{h(number)} = 25 \pm 6$  nm. (c) TEM image of **6**:  $D_{av} = 16 \pm 2$  nm, after counting more than 150 nanoparticles. (d) DLS results of **6**:  $D_{h(intensity)} = 125 \pm 129$  nm,  $D_{h(volume)} = 24 \pm 15$  nm and  $D_{h(number)} = 16 \pm 5$  nm.



### Scheme 1.

Synthetic route for the preparation of alkyne-functionalized PBYP<sub>49</sub>-*b*-PLLA<sub>44</sub>, **2**, by one pot-sequential ROP, followed by post-polymerization modifications *via* thiol-yne "click"-reactions using either 3-mercaptopropionic acid or 2-aminoethanethiol to prepare aPPE<sub>49</sub>-*b*-PLLA<sub>44</sub>, **3**, and cPPE<sub>49</sub>-*b*-PLLA<sub>44</sub>, **4**, respectively, and finally, schematic illustration of the assembly of **3** and **4** into spherical micelles by direct dissolution in water to afford anionic and cationic micelles, **5** and **6**, respectively (aPPE = anionic PPE and cPPE = cationic PPE).